Aalto University

Aaltodoc
OPEN ACCESS

This is an electronic reprint of the original article.
This reprint may differ from the original in pagination and typographic detail.

Author(s): Lindroos, Jeanette & Fenning, David P. & Backlund, Daniel J. & Verlage, Erik & Gorgulla, Angelika & Estreicher, Stefan K. & Savin, Hele & Buonassisi, Tonio

Title: Nickel: A very fast diffuser in silicon

Year: 2013

Version: Final published version

Please cite the original version:

Lindroos, Jeanette & Fenning, David P. & Backlund, Daniel J. & Verlage, Erik & Gorgulla, Angelika & Estreicher, Stefan K. & Savin, Hele & Buonassisi, Tonio. 2013. Nickel: A very fast diffuser in silicon. Journal of Applied Physics. P. 7. 0021-8979 (printed). DOI: 10.1063/1.4807799.

Note: Copyright 2013 American Institute of Physics. This article may be downloaded for personal use only. Any other use requires prior permission of the author and the American Institute of Physics. http://scitation.aip.org/content/aip/journal/jap

All material supplied via Aaltodoc is protected by copyright and other intellectual property rights, and duplication or sale of all or part of any of the repository collections is not permitted, except that material may be duplicated by you for your research use or educational purposes in electronic or print form. You must obtain permission for any other use. Electronic or print copies may not be offered, whether for sale or otherwise to anyone who is not an authorised user.

AIP Journal of Applied Physics

Nickel: A very fast diffuser in silicon

J. Lindroos, D. P. Fenning, D. J. Backlund, E. Verlage, A. Gorgulla, S. K. Estreicher, H. Savin, and T. Buonassisi

Citation: Journal of Applied Physics **113**, 204906 (2013); doi: 10.1063/1.4807799
View online: http://dx.doi.org/10.1063/1.4807799
View Table of Contents: http://scitation.aip.org/content/aip/journal/jap/113/20?ver=pdfcov
Published by the AIP Publishing

Articles you may be interested in

Molecular adsorption on silicon (001): A systematic evaluation of size effects in slab and cluster models
AIP Advances **3**, 042117 (2013); 10.1063/1.4802837

Communication: A new ab initio potential energy surface for HCl–H2O, diffusion Monte Carlo calculations of D 0 and a delocalized zero-point wavefunction
J. Chem. Phys. **138**, 121102 (2013); 10.1063/1.4799231

Structure, stability, and diffusion of arsenic-silicon interstitial pairs
Appl. Phys. Lett. **87**, 231905 (2005); 10.1063/1.2130398

Multiscale modeling of stress-mediated diffusion in silicon: Ab initio to continuum
Appl. Phys. Lett. **78**, 201 (2001); 10.1063/1.1336158

Boron diffusion in silicon in the presence of other species
Appl. Phys. Lett. **77**, 2683 (2000); 10.1063/1.1320019

[This article is copyrighted as indicated in the article. Reuse of AIP content is subject to the terms at: http://scitation.aip.org/termsconditions. Downloaded to] IP: 130.233.216.27 On: Thu, 09 Apr 2015 07:11:35

Nickel: A very fast diffuser in silicon

J. Lindroos,[1,a),b)] D. P. Fenning,[2] D. J. Backlund,[3] E. Verlage,[2,c)] A. Gorgulla,[4,a)] S. K. Estreicher,[3] H. Savin,[1] and T. Buonassisi[2,d)]
[1]*Department of Micro and Nanosciences, Aalto University, Tietotie 3, 02150 Espoo, Finland*
[2]*Department of Mechanical Engineering, Massachusetts Institute of Technology, 77 Massachusetts Avenue, Cambridge, Massachusetts 02139, USA*
[3]*Department of Physics, Texas Tech University, Lubbock, Texas 79409-1051, USA*
[4]*Department of Physics, University of Konstanz, Jacob-Burckhardt-Str. 29, 78464 Konstanz, Germany*

(Received 12 March 2013; accepted 10 May 2013; published online 29 May 2013)

Nickel is increasingly used in both IC and photovoltaic device fabrication, yet it has the potential to create highly recombination-active precipitates in silicon. For nearly three decades, the accepted nickel diffusivity in silicon has been $D_{Ni}(T) = 2.3 \times 10^{-3}\exp(-0.47\ \text{eV}/k_BT)\ \text{cm}^2/\text{s}$, a surprisingly low value given reports of rapid nickel diffusion in industrial applications. In this paper, we employ modern experimental methods to measure the higher nickel diffusivity $D_{Ni}(T) = (1.69 \pm 0.74) \times 10^{-4}\exp(-0.15 \pm 0.04\ \text{eV}/k_BT)\ \text{cm}^2/\text{s}$. The measured activation energy is close to that predicted by first-principles theory using the nudged-elastic-band method. Our measured diffusivity of nickel is higher than previously published values at temperatures below 1150 °C, and orders of magnitude higher when extrapolated to room temperature. © *2013 AIP Publishing LLC*. [http://dx.doi.org/10.1063/1.4807799]

I. INTRODUCTION

Unintentional nickel contamination is often present in silicon-based IC[1] and solar-cell[2,3] devices, as nickel can easily be introduced to the silicon wafer surface (e.g., from stainless steel components) at any step of the manufacturing process and further diffuse into the wafer during high-temperature processing. Nickel is also difficult to remove from the wafer surface with standard RCA cleanings or Si etching, as it appears to replate to the wafer surface during wet chemical processing.[4] Recently, the use of nickel components has increased in different device-manufacturing stages including silicon refining, wafer sawing, and metallization. Nickel alloys are used in CVD reactor coating materials for polysilicon manufacturing.[5–7] Nickel is present in the wafer cutting wire, but the contamination risk is much higher in nickel-coated diamond wire.[8] In polysilicon thin-film transistors, nickel induced lateral crystallization[9] is applied to crystallize amorphous silicon. In CMOS structures, nanoscale nickel silicide wiring[10] is studied as a replacement for copper contacts. In silicon solar cells, electroplated nickel and copper contacts[11] are considered as replacements for expensive silver-pasted front contacts, which could reduce cell fabrication costs[12] but also decrease cell efficiency due to contamination of fast diffusers. For example, a non-uniform ohmic nickel silicide diffusion barrier layer is reported to cause emitter shunting in copper-contacted Czochralski (Cz) silicon solar cells.[13,14]

The device impacts of nickel are closely related to its point-defect transport properties and precipitate characteristics. Since interstitial nickel (Ni_i) has both high solid solubility[15] and diffusivity, it is easily introduced into silicon at elevated temperatures. Rapid quenching causes the dissolved Ni_i to precipitate easily, due to the small lattice mismatch between silicon and nickel silicide ($NiSi_2$)[16,17] and the neutral charge state of Ni_i.[15] $NiSi_2$ precipitates are highly recombination active:[18] Minority carrier lifetime reduction is reported in *n*-type[19] Cz silicon with Ni concentrations of $1 \times 10^{11}\ \text{cm}^{-2}$, and in *p*-type[20] as low as $3 \times 10^{10}\ \text{cm}^{-2}$, correspondingly. Synchrotron measurements in *p*-type silicon have also directly confirmed the recombination activity at $NiSi_2$ precipitates.[21] In modern multi-crystalline silicon (mc-Si) solar cells, feedstock nickel contamination levels of $3 \times 10^{17}\ \text{cm}^{-3}$ increase emitter recombination and also decrease blue response,[2] presumably due to Ni out-diffusion to or near the front surface during cooling.[22]

Although preliminary reports from IC manufacturers suggest that neutral Ni_i^0 appears to diffuse as rapidly as positively charged Cu_i^+, there is no agreement on the exact diffusivity of interstitial nickel in crystalline silicon. In previous experimental studies,[23,24] the reported activation energies vary from 0.13 to 4.24 eV, while the pre-exponential coefficient ranges from 10^{-13} to 0.5 cm^2/s. These large discrepancies in the measured diffusivity could originate from several sources of experimental error. In studies conducted prior to the 1980s, it is typical that scarce information is provided regarding the annealing conditions, non-oxidizing annealing atmosphere, sample characteristics, and quenching rates. Control of the annealing temperature is crucial to minimize errors in estimating the solubility and diffusivity in experiments that measure the solubility-diffusivity product (i.e., most experiments involving radiotracers[23,25–27] and Rutherford Backscattering Spectrometry[28]). Because of the

[a)]Visiting researchers at Massachusetts Institute of Technology, Cambridge, Massachusetts 02139, USA.
[b)]E-mail: jeanette.lindroos@aalto.fi
[c)]Present address: California Institute of Technology, Pasadena, California 91125, USA.
[d)]E-mail: buonassisi@mit.edu

 © 2013 AIP Publishing LLC

[This article is copyrighted as indicated in the article. Reuse of AIP content is subject to the terms at: http://scitation.aip.org/termsconditions. Downloaded to] IP: 130.233.216.27 On: Thu, 09 Apr 2015 07:11:35

low nucleation energy barrier for $NiSi_2$ formation, a temporally invariant annealing temperature is essential to exclude the possibility of periodic Ni_i precipitation and re-dissolution during oscillating temperature decreases and increases, respectively, else the observed (effective, time-averaged) diffusivities may be lower. Bulk defects may also contribute to lower measured diffusivities; most previous studies were performed on Cz silicon with unreported oxygen and stacking fault concentrations.

The most commonly used diffusivity is $D_{Ni}(T) = 2.3 \times 10^{-3} \exp(-0.47\ \text{eV}/k_BT)\,\text{cm}^2/\text{s}$, reported by Bakhadyrkhanov *et al.*[26] However, the present authors have several concerns with this result. First, the available abstract[26] does not specify the choice of material, annealing equipment, and diffusion conditions. In addition, the activation energy of 0.47 eV differs by more than a factor of two from the activation energy of 0.21 eV (Refs. 29 and 30) obtained from first-principles calculations using the nudged-elastic-band[31,32] (NEB) method. The predicted Ni_i activation energy for diffusion of 0.21 eV is very close to that reported by Istratov *et al.*[33] for Cu_i^+, 0.18 ± 0.01 eV, which itself matches the one calculated[30] with NEB. A small Ni_i activation energy is indeed expected, since the electronic structure and atomic radius of Ni_i^0 are similar to that of Cu_i^+, and the elastic strain energy term tends to dominate the activation energy. Thus, it is unlikely for the activation energy for diffusion of Ni_i in Si to be as large as 0.47 eV. Finally, and perhaps most concerning, the solubility obtained by Bakhadyrkhanov *et al.*[26] is four orders of magnitude lower than the established Ni solubility[15] at 900°C.

In this paper, we measure anew the nickel diffusivity in high-quality intrinsic Float Zone (FZ) silicon. Section II presents the theoretical predictions for the migration path and activation energy for diffusion of Ni_i and its interaction with common defects in silicon. Section III details the accumulation and the direct diffusion experiments devised for measuring the diffusivity of nickel in silicon. The results are discussed in Sec. IV.

II. THEORETICAL PREDICTIONS

A. Methodology

The first-principles electronic structure and *ab-initio* molecular-dynamics simulations[34] are based on the SIESTA method.[35,36] The host crystal is represented by periodic supercells containing 216 host atoms. The defect geometries are obtained with a conjugate gradient algorithm. A $3 \times 3 \times 3$ Monkhorst-Pack[37] mesh is used to sample the Brillouin zone.

The gap levels are evaluated using the marker method.[38,39] The perfect crystal is used as the marker: The reference donor and acceptor levels are the top of the valence band and the bottom of the conduction band, respectively. This works well[29,40] for a wide range of defects provided that a $3 \times 3 \times 3$ k-point sampling is used and the lattice constant of the supercell is optimized in each charge state.

The electronic core regions are described using *ab-initio* norm-conserving pseudopotentials with the Troullier-Martins parameterization[41] in the Kleinman-Bylander form.[42] The SIESTA pseudopotentials are optimized using the experimental bulk properties of perfect solids and first-principles calculations[43] as well as measured vibrational properties of free molecules or known defects when such data are available.

The electronic valence regions are described using density-functional theory within the generalized gradient approximation for the exchange-correlation potential.[44] The charge density is projected on a real-space grid with an equivalent cutoff of 350Ryd to calculate the exchange-correlation and Hartree potentials. The basis sets for the valence states are linear combinations of numerical atomic orbitals:[45,46] Double-zeta (two sets of valence s and p's) for H, C, and O to which polarization functions (one set of d's) are added for Si. The basis sets of Ni include two sets of s and d orbitals, and one set of p's.

B. Properties of Ni_i

The lowest-energy configuration for Ni_i is at the tetrahedral interstitial (T) site with a very small outward relaxation of the four Si nearest neighbors. The Ni_i–Si distance is 2.438 Å, while the T-site to Si distance in the perfect crystal is 2.367 Å. The Ni-Si overlap population is very small, 0.06, a value consistent with negligible covalent Ni_i–Si interactions.

No gap levels associated with of isolated Ni_i have been reported in the literature. Our calculations[29] show that Ni_i has no level in the gap and that Ni_i thus remains in the same charge state for all positions of the Fermi level. Further, the position of the calculated donor level is below the top of the valence band and the position of the calculated acceptor level is just above the bottom of the conduction band. Therefore, the charge state of Ni_i is always 0. Ni_i^0 has spin 0 (the spin 1 state is about 1 eV higher in energy).

The migration path and activation energy for diffusion of Ni_i have been calculated[29,30] with the NEB[31,32] method in a 64 host-atoms cell and a $2 \times 2 \times 2$ mesh. Seven images were used, as shown in Fig. 1. The migration path between neighboring T sites is along the trigonal axis. The activation

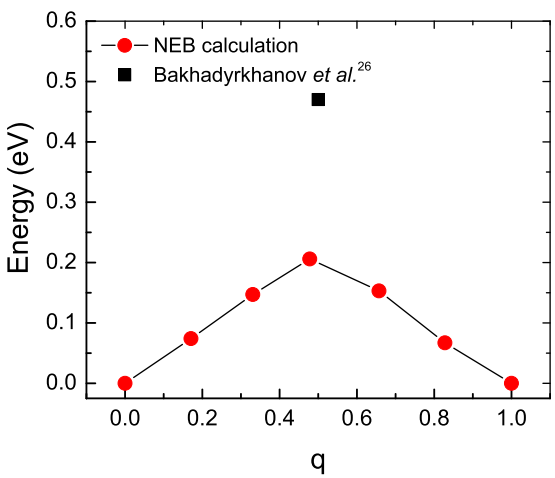

FIG. 1. Nudged-elastic-band calculation of the (T site to T site) diffusion barrier of Ni_i in Si along the generalized coordinate, q. The generally accepted value for nickel activation energy reported by Bakhadyrkhanov *et al.*[26] is shown for comparison.

[This article is copyrighted as indicated in the article. Reuse of AIP content is subject to the terms at: http://scitation.aip.org/termsconditions. Downloaded to] IP: 130.233.216.27 On: Thu, 09 Apr 2015 07:11:35

energy for diffusion with the pbe[44] and r-pbe[47] functionals is 0.21 eV.

C. Interactions of Ni_i with defects

The early diffusion experiments[48] for Cu_i^+ in Si used B-doped Si to produce high concentrations of copper in the sample. The measured activation energy for diffusion, 0.43 eV, turned out to be that of Cu_i^+ hopping from B^- to B^- rather than that of isolated Cu_i^+ in defect-free material. Hartree-Fock calculations[49] in clusters predicted an upper limit of 0.24 eV for this migration barrier. Transient-ion drift experiments[33] showed that this barrier is 0.18 ± 0.01 eV, and more recent NEB calculations in supercells[30] predict 0.18 eV as well. This illustrates the importance of considering possible traps for Ni_i which could affect the experimental measurements. Note that the binding energies of Ni_i to a defect X are calculated at $T = 0$ K. These values drop as the temperature increases[50,51] as the configurational entropy drives Ni_i away from X (such an effect has been observed in the case of H_2 molecules in Si trapped near interstitial oxygen[52,53]).

Since Ni_i is always in the 0 charge state, there is no long-range Coulomb attraction to shallow dopants. The dominant impurities in the high-resistivity FZ silicon material used here are substitutional C (C_s) and interstitial O (O_i). But there is also Ni_i in the material during the diffusion experiments, and possibly interstitial H, which could be present in the metallic Ni deposited on the surface and diffuse into the bulk during the anneal. The concentrations of native defects in the sample are very low, and the annealing temperatures are too low to generate meaningful quantities of Frenkel pairs. Therefore, the concentration of Si self-interstitials (I_{Si}) and vacancies (V) in the samples under the experimental conditions is too low to affect the migration of Ni_i.

The interaction between Ni_i and C_s is repulsive by 0.31 eV. Thus, C_s does not interfere with the diffusion of Ni_i. The interaction between Ni_i and O_i is attractive but very weak: 0.07 eV. This trap energy is smaller than the 0.21 eV activation energy for diffusion calculated at the same level of theory. Therefore, O_i does not interfere with the diffusion of Ni_i. Ni_i–Ni_i interactions result in a very weakly bound trigonal pair that is only 0.06 eV lower in energy than two isolated Ni_i's in Si. Thus, the interactions between isolated Ni_i's can be ignored as well.

Ni_i weakly interacts with bond-centered hydrogen H_{bc}^+, the stable state in *p*-type and intrinsic Si.[40,54] No Ni–H bond forms but Ni_i is 0.24 eV more stable[55] near H_{bc}^+ than far away from it. Indeed, the Si-Si bond relaxes when forming Si-H-Si and this increases the volume available at the adjacent interstitial sites. This extra space lowers the energy of Ni_i. As mentioned above, the 0.24 eV binding energy is calculated at $T = 0$ K and becomes smaller at higher temperatures, and H does not interfere with the diffusion of Ni_i. Thus, under the present experimental conditions, no trap-limited diffusion of Ni_i is expected.

For completeness, we have also calculated the interactions of Ni_i with I_{Si}^0 and V^0. There are two weakly bound {Ni,I_{Si}} pairs: 0.39 and 0.25 eV, respectively. The interaction of Ni_i with V^0 is much more energetic,[29] as Ni becomes substitutional and forms four Ni-Si covalent bonds: $Ni_i + V^0 \rightarrow Ni_s + 2.60$ eV.

III. EXPERIMENTS

A. Constraints and sources of error in nickel diffusivity measurements

Measuring the diffusivity of nickel in Si is challenging, primarily since Ni_i is a very fast diffuser, even during sample cooling. Consequently, radiotracer methods have proven largely ineffective at quantifying diffusion profiles, as nickel in intentionally contaminated samples tends to be either homogeneously distributed or out-diffused to the surface.[22] In addition, Ni_i diffuses without a charge and does not form nickel-acceptor pairs, as opposed to iron and copper,[56] preventing the use of sensitive electrical characterization methods such as recombination lifetime or transient ion drift[57] measurements. Nickel is known to precipitate at oxygen precipitates[58,59] and extended defects,[60] highlighting the importance of using high-quality silicon in diffusivity measurements. As the $NiSi_2$ precipitates easily upon cooling,[16,17] a slight fluctuation of the annealing temperature could force heterogeneous nickel precipitation, resulting in a measured diffusivity value that is lower than the actual Ni_i diffusivity. Therefore, good temperature stability is required during nickel in-diffusion annealing.

Fast sample heating and cooling are also necessary to ensure that the diffusion profile is not distorted during the temperature ramps. The high diffusivity of Ni_i requires the use of a very thick sample (several centimeters) even for short annealing times, in order to achieve the direct Ni_i diffusion profile in a semi-infinite medium. Unfortunately, the large thermal mass of such a thick sample inhibits fast ramping. This is especially problematic during quenching, as too rapid quenching leads to large thermal gradients and sample fracture, while too slow cooling risks the out-diffusion on nickel.

Finally, a large temperature range is needed to reliably fit the measured diffusivity data. This is also challenging, since the Ni detection limit of the measurement tool determines the lowest possible temperature based on Ni solubility. On the high temperature end, the Si:Ni phase change at 964°C alters the boundary phase, thus changing the solubility.

Therefore, the experimental window is narrow for the combination of sample thickness, annealing temperature range, annealing time, and ramping rates. In order to optimize these parameters and reliably determine the diffusivity of nickel, we have performed both "accumulation" as well as "direct diffusion" experiments. The methodologies and sample preparation of both methods are discussed below.

1. Accumulation experiments

In the accumulation experiments forthwith, the diffusivity of Ni_i is obtained by measuring the linear accumulation of nickel from a $NiSi_2$ "infinite source" (formed from an evaporated Ni layer) to an infinite "sink" or gettering layer

[This article is copyrighted as indicated in the article. Reuse of AIP content is subject to the terms at: http://scitation.aip.org/termsconditions. Downloaded to] IP: 130.233.216.27 On: Thu, 09 Apr 2015 07:11:35

(e.g., liquid aluminum-silicon layer).[28] Once the sample has reached a stable temperature, steady-state diffusion is established in the sample due to the high Ni_i diffusivity, infinite Ni source, and infinite Al-Si sink. Therefore, the flux of Ni atoms J_{Ni} through a silicon sample of thickness d is $J_{Ni} = DS/d$, where D is the diffusivity and S the solubility of Ni. The number of Ni atoms N transported through the sample and accumulated in the infinite Al-Si sink is $N = J_{Ni}t = DSt/d$, assuming perfect segregation, which is a valid approximation before saturation of the gettering layer. By measuring the accumulated Ni concentration N in the Al-Si sink as a function of time, the diffusivity can be extracted from the slope DS/d, as the solubility S and sample thickness d are known.

There are several advantages to the accumulation experiment compared to the direct diffusion experiment. First, the temperature range is only limited by the eutectic temperature of Si:Al (577°C) and Si:Ni (964°C). Although $NiSi_2$ starts to transform into NiSi at temperatures below 800°C,[61] the phase does not appear to affect nickel solubility[15] in silicon at temperatures above 500°C. The accumulation of Ni in the Al-Si sink allows for longer annealing times than in the direct diffusion experiment, reducing the effect of the sample heat-up time. The detection limit of the Ni characterization method is also less crucial. However, longer annealing times require long-time stability of the annealing conditions. This was established by measuring the annealing temperature with a thermocouple and the sample temperature with two different optical pyrometers. With these temperature controls, the error in absolute temperature was established to be lower than 5°C and the fluctuations in temperature during annealing lower than 1.5°C. We observed that optimal tube positioning within the furnace and care to ensure unidirectional airflow is crucial to ensure stable operating temperatures.

The accumulation experiment was performed on ⟨100⟩ oriented 4380–5230 Ω cm FZ silicon. First, samples of 17×17 mm^2 were laser cut from the wafers. The samples were then cleaned with standard RCA 1 and RCA 2 cleanings, followed by a 30 s HF dip. Next, 150 nm of Ni was deposited with an e-beam evaporator over an area of 7×7 mm^2 on the sample front side, while 1 μm of Al was evaporated onto the same area on the back surface. The samples were annealed in a vertical tube furnace in forming gas with a flow rate of 3 scfh. The sample load time was 25 s, after which the annealing temperature was reached in about 1 min. The Ni in-diffusion anneal was followed by a rapid quench (estimated 200°C/s)[62] in silicone oil. Finally, the samples were cleaned in acetone and the Ni concentration was measured in the Al-Si layer with a SPECTRO XEPOS X-Ray Fluorescence (XRF) spectrometer. An energy dispersive XRF measurement, a quantitative technique,[63] was performed in a 6 mm diameter spot on the Al-Si pad with a 50 W palladium X-ray tube using a molybdenum target. The Ni concentration in the Al-Si layer was obtained by calibrating the measurement result to the XRF spectra of a known Ni source. The XRF Ni detection limit is 1×10^{15} cm^{-2}.

To verify the experiment, several control samples were annealed and the Ni concentration measured with XRF. First, samples with an Al layer, but no Ni layer, were measured before and after annealing. As no Ni signal could be detected, any Ni present in the Al-Si layer after annealing will have arrived there by diffusion. Next, samples of two different Si thicknesses (430 and 680 μm) were annealed at 665±5°C and measured with XRF to test whether vapor-phase or surface diffusion of Ni occurred during annealing. The 430 μm sample was thinned from the 680 μm thick wafer, to ensure that doping and impurity concentrations were consistent between samples. The accumulation rate was found to depend on $1/d$ to within 7%, indicating that bulk diffusion is the dominant transport mechanism of nickel from the Ni source pad to the Al gettering layer, and that surface and vapor diffusion can be neglected.

After establishing bulk diffusion, the accumulation experiment was performed at six in-diffusion temperatures in the range of 665−885°C. At each in-diffusion temperature, four samples with Si thickness 680 μm were annealed from 10 min to 8 h in order to measure Ni concentration in the Al-Si layer as a function of annealing time.

2. Direct diffusion experiments

The purpose of the direct diffusion experiment is to measure the nickel concentration profile in silicon resulting from Ni diffusion from an infinite $NiSi_2$ source into a semi-infinite medium of silicon. To achieve the criteria for a semi-infinite diffusion for the fast-diffusing Ni_i, the experiment was performed on 3.2 cm thick 3500–4000 Ω cm FZ silicon with approximately 6 ppta B and 26 ppta P doping.

A sample of $3.2 \times 3.2 \times 3.2$ cm^3 was first cut with a tile saw and subjected to mechanical polishing, removing 3 mm from the length, thickness, and depth of the sample. The sample was then cleaned using a 1.5 min surface etch in 1:100 mixture of HF and HNO_3, standard RCA1 and RCA2 processes and a 30 s HF dip. Next, 150 nm of Ni was deposited with an e-beam evaporator onto the ⟨100⟩ oriented front surface of the sample. The sample was subsequently annealed for 28 min in a vertical tube furnace in forming gas (3 scfh) at 885°C. The annealing temperature was measured with a thermocouple and the sample temperature with two pyrometers. The sample heat-up time was measured as 8 min, which corresponds to the heat-up profile obtained with Abaqus simulation. After 20 min of annealing at target temperature, the sample was quenched by forced air cooling, as liquid quenching would have caused the sample to shatter. After 2 min of forced air cooling, the sample surface temperature had dropped to 155°C and room-temperature was reached within 19 min.

Next, a smaller sample was prepared from the annealed sample for Secondary Ion Mass Spectrometry (SIMS) profiling. The smaller sample was cut parallel to the Ni surface in order to measure the Ni concentration as a function of sample depth near the $NiSi_2$ source layer. After polishing, the $15 \times 7.5 \times 4.5$ mm^3 sample was etched in 3:1 HCl:HNO_3 for 1.5 h to remove the evaporated Ni layer and then for 1.5 min in 1:100 HF:HNO_3 to undercut and remove residual surface contamination without significantly reducing the sample size. Finally, the ^{60}Ni concentration was measured at the

[This article is copyrighted as indicated in the article. Reuse of AIP content is subject to the terms at: http://scitation.aip.org/termsconditions. Downloaded to] IP: 130.233.216.27 On: Thu, 09 Apr 2015 07:11:35

National Renewable Energy Laboratory (NREL) by dynamic SIMS with a 10 keV O_2^+ primary ion source with a 30 μm diameter beam spot size rastered over an area from 60 × 60 to 500 × 500 μm^2 on the 15 × 7.5 × 4.5 mm^3 sample.

IV. RESULTS AND DISCUSSION

Figure 2 presents the Ni concentration measured with XRF in the Al-Si sink layer as a function of annealing time at six in-diffusion temperatures in the accumulation experiment. The annealing time refers to the time interval from sample heat-up (after loading) to quenching, and has an error of 1 min, due to sample heat-up time. The error in the measured Ni concentration is obtained from the XRF quantification uncertainty.

For each in-diffusion temperature, the Ni concentration as a function of time was fitted linearly with the least square estimation (LSE) method by York *et al.*,[64] taking into account the measurement errors on both axes. The slope of these fits corresponds to the Ni flux $J_{Ni} = DS/d$ through the Si sample at each diffusion temperature. The diffusivity D at each temperature and its corresponding uncertainty was obtained from the slope DS/d, assuming that both the solubility[15] $S_{Ni}(T) = 1.227 \times 10^{24} \exp(-1.68\ \text{eV}/k_BT)\ \text{cm}^{-3}$ and the Si sample thickness are free of error. Table I summarizes both the DS/d values from the LSE fitting and the extracted diffusivity D values.

Figure 3 shows the obtained Ni flux DS/d as a function of the temperature with a 5 K temperature error. After a logarithmic transformation of the diffusivity data to perform an

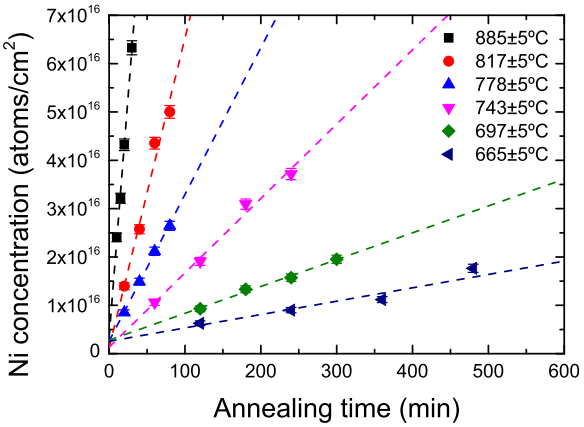

FIG. 2. Nickel concentration in the Al-Si layer as a function of annealing time in the accumulation experiment.

TABLE I. The Ni flux DS/d and the diffusivity D measured in the accumulation experiment.

Temperature (°C)	DS/d (atoms/cm^2 s)	Diffusivity D (cm^2/s)
665 ± 5	(4.61 ± 0.40) × 10^{11}	(2.72 ± 0.30) × 10^{-5}
697 ± 5	(9.25 ± 0.89) × 10^{11}	(2.75 ± 0.14) × 10^{-5}
743 ± 5	(2.56 ± 0.11) × 10^{12}	(3.06 ± 0.19) × 10^{-5}
778 ± 5	(5.06 ± 0.30) × 10^{12}	(3.19 ± 0.13) × 10^{-5}
817 ± 5	(1.07 ± 0.44) × 10^{13}	(3.47 ± 0.26) × 10^{-5}
885 ± 5	(3.31 ± 0.27) × 10^{13}	(3.76 ± 0.24) × 10^{-5}

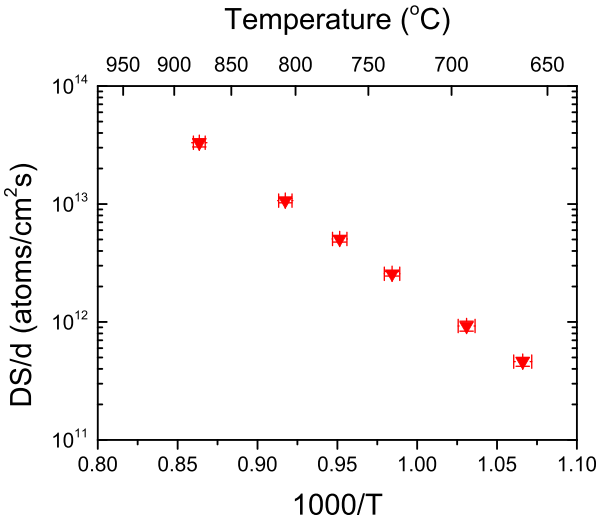

FIG. 3. Ni flux DS/d as a function of temperature in the accumulation experiment.

Arrhenius analysis, the activation energy and pre-exponential factor were extracted from the slope and intercept of the diffusivity data by another linear LSE.[64] Figure 4 presents the final diffusivity result $D_{Ni}(T) = (1.69 \pm 0.74) \times 10^{-4} \exp(-0.15 \pm 0.04\ \text{eV}/k_BT)\ \text{cm}^2/\text{s}$ obtained in the temperature range of 665–885°C. The error in the activation energy 0.04 eV and the pre-exponential error 0.74 × 10^{-4} cm^2/s are obtained from the uncertainty of the regression analysis.

This new diffusivity value is close to the previously established diffusivity[19] at temperatures above 900°C, but by 500°C, our result is one order of magnitude higher than the previously accepted value. The new activation energy for diffusion, 0.15 ± 0.04 eV, is significantly lower than the accepted value of 0.47 eV (Ref. 26) and corresponds rather well to the calculated[29,30] 0.21 eV. Hence, we conclude that the new diffusivity result better reflects the diffusivity of Ni_i in silicon than the previously obtained experimental values.[23,24]

Figure 5 shows the total Ni concentration (isotope correction factor applied) as a function of depth measured by

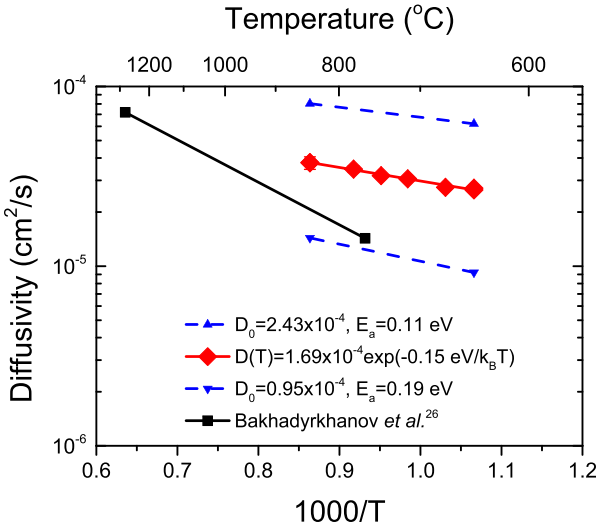

FIG. 4. Diffusivity of Ni_i in silicon measured in the accumulation experiment.

[This article is copyrighted as indicated in the article. Reuse of AIP content is subject to the terms at: http://scitation.aip.org/termsconditions. Downloaded to] IP: 130.233.216.27 On: Thu, 09 Apr 2015 07:11:35

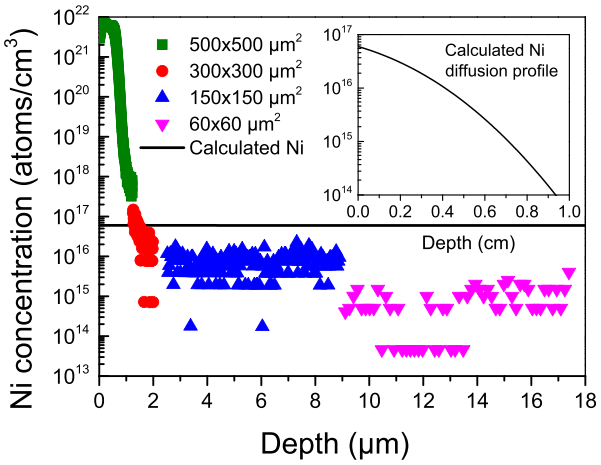

FIG. 5. Ni concentration measured as a function of depth with dynamic SIMS in the direct diffusion experiment. The raster size was decreased from 500×500 to 60×60 μm^2 with increasing depth to eliminate the effect of residual surface Ni. Inset: The calculated Ni diffusion profile assuming perfect quenching.

SIMS in the direct diffusion experiment. The SIMS analysis area is a 60 μm diameter spot in the center of the rastered area of 60×60 to 500×500 μm^2. The inset of Fig. 5 displays the calculated Ni diffusion profile for 20 min annealing at 885°C based on the accumulation experiment diffusivity result, assuming perfect quenching. The high Ni concentration measured near the sample surface is most likely caused by the insufficient removal of evaporated Ni and nickel silicide prior to measurement. Therefore, to prevent surface Ni from affecting the measurement, the rastered area is reduced as a function of depth from 500×500 to 60×60 μm^2. Already 2 μm into the sample, the measured Ni concentration is lower than the expected value, and the Ni concentration continues to decrease as a function of depth until the detection limit is reached.

Clearly, the Ni concentration obtained with SIMS does not correspond to the calculated profile based on our new value for Ni_i diffusivity—nor to any profile based on a peer-reviewed, literature-reported diffusivity value.[23,24] Instead, the measured Ni profile appears rather to mimic the out-diffusion of Ni. As the chosen FZ silicon material does not contain heterogeneous nucleation sites for Ni precipitates and nickel prefers to diffuse to the Si surface,[22] out-diffusion of Ni during sample cooling or subsequent sample polishing is the most likely cause for the low measured concentration of nickel. Therefore, obtaining the Ni diffusivity via a direct diffusion experiment requires a more carefully co-optimized selection of the bulk heterogeneous nucleation site density, sample thickness, sample quenching rate, and sample preparation prior to Ni measurement. The complexity of designing such an experiment highlights the challenges of accurately measuring Ni diffusivity, and may account for some of the large diversity of diffusivity values in the literature.[23,24]

V. CONCLUSIONS

Given the multiple challenges associated with accurately measuring the diffusivity of Ni_i in silicon, the twelve orders of magnitude variation reported in the literature[23,24] is not entirely surprising. Since Ni_i^0 has similar size and electronic structure as Cu_i^+ in *p*-type and intrinsic Si, it is intuitive to expect that their intrinsic diffusion coefficients should also be similar. The long-accepted 0.47 eV (Ref. 26) activation energy for diffusion of Ni_i is, in fact, close to old textbook value for Cu_i^+, 0.43 eV,[48] which was later shown[33] to be associated with the trap-limited diffusion of Cu_i^+ in heavily B-doped Si. In low-doped material, Cu_i^+ diffuses with a 0.18 ± 0.01 eV (Ref. 33) activation energy, a value which matches the most recent NEB calculations.[30] As expected, this activation energy Cu_i^+ is similar to our measured 0.15 ± 0.04 eV for Ni_i^0, which is close to the 0.21 eV predicted by NEB calculations.[29,30]

The direct diffusion experiment did not provide an easily recognizable Ni diffusion profile, as the slow sample cooling most likely caused Ni to out-diffuse before SIMS measurements. In the accumulation experiment, the nickel diffusivity of $D_{Ni}(T) = (1.69 \pm 0.74) \times 10^{-4} \exp(-0.15 \pm 0.04 \text{ eV}/k_BT)\,\text{cm}^2/\text{s}$ was obtained by measuring the linear accumulation of Ni in an infinite Al-Si sink.

At lower temperatures, the new diffusion coefficient is larger than the established diffusivity, which emphasizes the importance of avoiding Ni contamination in silicon-based device manufacturing. In solar cells with nickel- and copper-plated front contacts, even short back-contact firing steps can cause Ni contamination during contact formation and Ni precipitation upon rapid cooling. Although Ni solubility might change at low temperatures (below 400°C) due to Ni_2Si and NiSi boundary phase changes, once Ni has been introduced into Si, the high diffusivity allows interstitial Ni to stay mobile during slow cooling and easily diffuse into the wafer bulk. Nevertheless, the high diffusivity of Ni_i could also be used to remove Ni from contaminated silicon wafers. By creating appropriate external Ni precipitation sites and using low-temperature annealing with slow cooling, Ni contamination could be gettered from the bulk to selected in-active surface regions, efficiently reducing the deleterious nickel concentration in the silicon-based device.

ACKNOWLEDGMENTS

We acknowledge A. A. Istratov (Siltronic) for providing high-purity Float Zone silicon; R. Reedy (NREL) for providing SIMS measurements; H. J. Choi for providing XRF assistance, D. M. Powell for sample heating-rate simulations, and V. Modi for furnace temperature profiling. This research was supported primarily by the U.S. Department of Energy under Contract No. DE-EE0005314. The work of S.K.E. is supported in part by the Grant No. D-1126 from the R. A. Welch Foundation. J.L. acknowledges the support of the Fulbright-Technology Industries of Finland Grant and the Ernst Wirtzen Fund, and D.P.F. an NSF Graduate Research Fellowship. This work was performed in part at the Harvard Center for Nanoscale Systems (CNS), a member of the National Nanotechnology Infrastructure Network (NNIN), which is supported by the National Science Foundation under NSF Award No. ECS-0335765. The High Performance

[This article is copyrighted as indicated in the article. Reuse of AIP content is subject to the terms at: http://scitation.aip.org/termsconditions. Downloaded to] IP: 130.233.216.27 On: Thu, 09 Apr 2015 07:11:35

Computer Center at Texas Tech provided generous amounts of computer time.

[1]K. Graff, *Metal Impurities in Silicon-Device Fabrication*, 2nd ed. (Springer, Berlin, 2000).
[2]G. Coletti, P. C. P. Bronsveld, G. Hahn, W. Warta, D. Macdonald, B. Ceccaroli, K. Wambach, N. Le Quang, and J. M. Fernandez, Adv. Funct. Mater. **21**, 879 (2011).
[3]T. Buonassisi, A. A. Istratov, M. D. Pickett, M. Heuer, J. P. Kalejs, G. Hahn, M. A. Marcus, B. Lai. Z. Cai, S. M. Heald, T. F. Ciszek, R. F. Clark, D. W. Cunnigham, A. M. Gabor, P. Jonczyk, S. Narayanan, E. Sauar, and E. R. Weber, Prog. Photovoltaics **14**, 513 (2006).
[4]T. Hosoya, Y. Ozaki, and K. Hirata, J. Electrochem. Soc. **132**, 2436 (1985).
[5]K. M. Jayakar and U. R. Kultgen, "Polycrystalline silicon production," WIPO patent 012457 (26 January 2012).
[6]J. S. S. Sanchez, J. L. M. Barona, E. A. Conejero, M. V. V. Canle, X. B. Rel, P. T. L. Garcia, and M. T. Martinez, "Fluidized bed reactor for production of high purity silicon," U.S. patent 8168123 (1 May 2012).
[7]R. Froehlich, B. Fieselmann, D. Mixon, and Y. Tsuo, "Reactor with silicide-coated metal surfaces," U.S. patent 0266466 (21 October 2010).
[8]M. Dhamrin, T. Saitoh, K. Kamisako, T. Mori, and N. Iwamoto, *in Proceedings of the 25th EU PVSEC, Valencia, Spain, 6-10 September* (2010), p. 1600.
[9]C. Hayzelden, J. L. Batstone, and R. C. Cammarata, Appl. Phys. Lett. **60**, 225 (1992).
[10]Y. Wu, J. Xiang, C. Yang, W. Lu, and C. M. Lieber, Nature **430**, 61 (2004).
[11]J. Bartsch, Ph.D. dissertation, University of Freiburg, Germany, 2011.
[12]D. M. Powell, M. T. Winkler, H. J. Choi, C. B. Simmons, D. Berney Needleman, and T. Buonassisi, Energy Environ. Sci. **5**, 5874 (2012).
[13]M. Aleman, N. Bay, D. Barucha, A. Knorz, D. Biro, R. Preu, and S. W. Glunz, in *Proceedings of the 24th EU PVSEC, Hamburg, Germany, 21-25 September* (2009), p. 1414.
[14]C. Boulord, A. Kaminski, Y. Veschetti, G. Poulain, D. Blanc-Pelissier, B. Grange, and M. Lemiti, in *Proceedings of the 25th EU PVSEC, Valencia, Spain, 6-10 September* (2010), p. 2215.
[15]A. A. Istratov, P. Zhang, R. J. McDonald, A. R. Smith, M. Seacrist, J. Moreland, J. Shen, R. Wahlich, and E. R. Weber. J. Appl. Phys. **97**, 023505 (2005).
[16]M. Seibt and W. Schröter, Philos. Mag. A **59**, 337 (1989).
[17]K. Ryoo, R. Drosd, and W. Wood, J. Appl. Phys. **63**, 4440 (1998).
[18]A. A. Istratov and E. R. Weber, Appl. Phys. A **66**, 123 (1998).
[19]Y. Yoon, B. Paudyal, J. Kim, Y. W. Ok, P. Kulshreshtha, S. Johnston, and G. Rozgonyi, J. Appl. Phys. **111**, 033702 (2012).
[20]H. Savin, M. Yli-Koski, A. Haarahiltunen, H. Talvitie, and J. Sinkkonen, ECS Trans. **11**, 319 (2007).
[21]T. Buonassisi, A. A. Istratov, M. D. Pickett, M. A. Marcus, G. Hahn, S. Riepe, J. Isenberg, W. Warta, G. Willeke, T. F. Ciszek, and E. R. Weber, Appl. Phys. Lett. **87**, 044101 (2005).
[22]M. B. Shabani, T. Yoshimi, S. Okuuchi, and H. Abe, Solid State Phenom. **57–58**, 81 (1997).
[23]F. H. M. Spit, D. Gupta, and K. N. Tu, Phys. Rev. B **39**, 1255–1260 (1989).
[24]*Landolt-Börnstein: Numerical Data and Functional Relationships in Science and Technology*, Group III: Condensed Matter Vol. 33A, edited by D. L. Beke (Springer, Berlin, 1998), pp. 2–143.
[25]H. P. Bonzel, Phys. Status Solidi B **20**, 493 (1967).
[26]M. K. Bakhadyrkhanov, S. Zainabidinov, and A. Khamidov, Sov. Phys. Semicond. **14**, 243 (1980).
[27]V. A. Uskov, A. B. Fedotov, A. I. Rodionov, and N. S. Dumarevskaya, Inorg. Mater. **20**, 989 (1984).
[28]R. D. Thompson, D. Gupta, and K. N. Tu, Phys. Rev. B **33**, 2636 (1985).
[29]D. J. Backlund and S. K. Estreicher, Phys. Rev. B **81**, 235213 (2010).
[30]S. K. Estreicher, D. J. Backlund, C. Carbogno, and M. Scheffler, Angew. Chem. **50**, 10221 (2011).
[31]G. Mills and H. Jonsson, Phys. Rev. Lett. **72**, 1124 (1994); H. Jonsson, G. Mills, and K. W. Jacobsen, in *Classical and Quantum Dynamics in Condensed Phase Simulations*, edited by B. J. Berne, G. Ciccotti, and D. F. Coker (World Scientific, Singapore, 1998), p. 385.
[32]G. Henkelman, B. P. Uberuaga, and H. Jonsson, J. Chem. Phys. **113**, 9901 (2000); G. Henkelman and H. Jonsson, J. Chem. Phys. **113**, 9978 (2000).
[33]A. A. Istratov, C. Flink, H. Heislmair, E. R. Weber, and T. Heiser, Phys. Rev. Lett. **81**, 1243 (1998).
[34]*Theory of Defects in Semiconductors*, edited by D. A. Drabold and S. K. Estreicher (Springer, Berlin, 2007).
[35]D. Sánchez-Portal, P. Ordejón, E. Artacho, and J. M. Soler, Int. J. Quantum Chem. **65**, 453 (1997).
[36]E. Artacho, D. Sánchez-Portal, P. Ordejón, A. García, and J. M. Soler, Phys. Status Solidi B **215**, 809 (1999).
[37]H. J. Monkhorst and J. D. Pack, Phys. Rev. B **13**, 5188 (1976).
[38]A. Resende, R. Jones, S. Öberg, and P. R. Briddon, Phys. Rev. Lett. **82**, 2111 (1999).
[39]J. P. Goss, M. J. Shaw, and P. R. Briddon, *in Theory of Defects in Semiconductors*, edited by D. A. Drabold and S. K. Estreicher (Springer, Berlin, 2007), p. 69.
[40]S. K. Estreicher, A. Docaj, M. B. Bebek, D. J. Backlund, and M. Stavola, Phys. Status Solidi A **209**, 1872 (2012).
[41]N. Troullier and J. L. Martins, Phys. Rev. B **43**, 1993 (1991).
[42]L. Kleiman and D. M. Bylander, Phys. Rev. Lett. **48**, 1425 (1982).
[43]V. L. Moruzzi and C. B. Sommers, *Calculated Electronic Properties of Ordered Alloys: A Handbook* (World Scientific, Singapore, 1995).
[44]J. P. Perdew, K. Burke, and M. Ernzerhof, Phys. Rev. Lett. **77**, 3865 (1996).
[45]O. F. Sankey and D. J. Niklevski, Phys. Rev. B **40**, 3979 (1989).
[46]O. F. Sankey, D. J. Niklevski, D. A. Drabold, and J. D. Dow, Phys. Rev. B **41**, 12750 (1990).
[47]B. Hammer, L. Hansen, and J. K. Norskov, Phys. Rev. B **59**, 7413 (1999).
[48]R. H. Hall and J. H. Racette, J. Appl. Phys. **35**, 379 (1964).
[49]D. E. Woon, D. S. Marynick, and S. K. Estreicher, Phys. Rev. B **45**, 13383 (1992).
[50]S. K. Estreicher, M. Sanati, D. West, and F. Ruymgaart, Phys. Rev. B **70**, 125209 (2004).
[51]M. Sanati and S. K. Estreicher, Phys. Rev. B **72**, 165206 (2005).
[52]R. E. Pritchard, M. J. Ashwin, J. H. Tucker, R. C. Newman, E. C. Lightowlers, M. J. Binns, S. A. McQuaid, and R. Falster, Phys. Rev. B **56**, 13118 (1997).
[53]R. C. Newman, R. E. Pritchard, J. H. Tucker, and E. C. Lightowlers, Phys. Rev. B **60**, 12775 (1999).
[54]C. G. Van de Walle, Y. Bar-Yam, and S. T. Pantelides, Phys. Rev. Lett. **60**, 2761 (1988); C. G. Van de Walle, P. J. H. Denteneer, Y. Bar-Yam, and S. T. Pantelides, Phys. Rev. B **39**, 10791 (1989).
[55]D. J. Backlund and S. K. Estreicher, Phys. Rev. B **82**, 155208 (2010).
[56]C. Flink, H. Feick, S. A. McHugo, W. Seifert, H. Hieslmair, T. Heiser, A. A. Istratov, and E. R. Weber, Phys. Rev. Lett. **85**, 4900 (2000).
[57]T. Heiser, S. McHugo, H. Heislmair, and E. R. Weber, Appl. Phys. Lett. **70**, 3576 (1997).
[58]A. Bazzali, G. Borinetti, R. Orizio, D. Gambaro, and R. Falster, Mater. Sci. Eng., B **36**, 85 (1996).
[59]H. Savin, M. Yli-Koski, A. Haarahiltunen, H. Talvitie, and J. Sinkkonen, Solid State Phenom. **131–133**, 183 (2007).
[60]T. S. Fell and P. R. Wilshaw, J. Phys. IV **1**, C6 (1991).
[61]L. J. Chen, *Silicide Technology for Integrated Circuits* (IEE, London, 2004).
[62]A. A. Istratov, H. Hedemann, M. Seibt, O. F. Vyvenko, W. Schröter, T. Heiser, C. Flink, H. Hieslmair, and E. R. Weber, J. Electrochem. Soc. **145**, 3889 (1998).
[63]J. H. Hubbell, P. N. Trehan, N. Singh, B. Chand, D. Mehta, M. L. Garg, R. R. Garg, S. Singh, and S. Puri, J. Phys. Chem. Ref. Data **23**, 339 (1994).
[64]D. York, N. M. Evensen, M. López Martínez, and J. De Basabe Delegado, Am. J. Phys. **72**, 367 (2004).

[This article is copyrighted as indicated in the article. Reuse of AIP content is subject to the terms at: http://scitation.aip.org/termsconditions. Downloaded to] IP: 130.233.216.27 On: Thu, 09 Apr 2015 07:11:35